

# On variations in the fine-structure constant and stellar pollution of quasar absorption systems

Y. Fenner<sup>1</sup>★, M. T. Murphy<sup>2</sup>★, B. K. Gibson<sup>1</sup>

<sup>1</sup>Centre for Astrophysics & Supercomputing, Swinburne University of Technology, Melbourne, Australia

<sup>2</sup>Institute of Astronomy, University of Cambridge, Madingley Road, Cambridge CB3 0HA, UK

Accepted —. Received —; in original form —

## ABSTRACT

At redshifts  $z_{\text{abs}} \lesssim 2$ , quasar absorption-line constraints on space-time variations in the fine-structure constant,  $\alpha$ , rely on the comparison of Mg II and Fe II transition wavelengths. One potentially important uncertainty is the relative abundance of Mg isotopes in the absorbers which, if different from solar, can cause spurious shifts in the measured wavelengths and, therefore,  $\alpha$ . Here we explore chemical evolution models with enhanced populations of intermediate-mass (IM) stars which, in their asymptotic giant branch (AGB) phase, are thought to be the dominant factories for heavy Mg isotopes at the low metallicities typical of quasar absorption systems. By design, these models partially explain recent Keck/HIRES evidence for a smaller  $\alpha$  in  $z_{\text{abs}} < 2$  absorption clouds than on Earth. However, such models also over-produce N, violating observed abundance trends in high- $z_{\text{abs}}$  damped Lyman- $\alpha$  systems (DLAs). Our results do not support the recent claim of Ashenfelter, Mathews & Olive (2004b) that similar models of IM-enhanced initial mass functions (IMFs) may simultaneously explain the HIRES varying- $\alpha$  data and DLA N abundances. We explore the effect of the IM-enhanced model on Si, Al and P abundances, finding it to be much-less pronounced than for N. We also show that the  $^{13}\text{C}/^{12}\text{C}$  ratio, as measured in absorption systems, could constitute a future diagnostic of non-standard models of the high-redshift IMF.

**Key words:** quasars: absorption lines – stars: AGB – nucleosynthesis

## 1 INTRODUCTION

In the past few years, evidence has emerged that the fine-structure constant,  $\alpha \equiv e^2/hc$ , may have been smaller in high-redshift quasar (QSO) absorption systems than the value measured today on Earth (e.g. Webb et al. 1999; Murphy et al. 2004, hereafter MFW04). A possible explanation for the lower-redshift half of this result is that the abundances of the heavy Mg isotopes ( $^{25}\text{Mg}$  and  $^{26}\text{Mg}$ ) in the absorbers are much higher, relative to that of  $^{24}\text{Mg}$ , than solar values. Recently, Ashenfelter, Mathews & Olive (2004a) proposed and expanded upon (Ashenfelter, Mathews & Olive 2004b, hereafter AMO04) a chemical evolution model with an initial mass function (IMF) strongly enhanced at intermediate masses (IMs), whereby highly super-solar abundances of heavy Mg isotopes are produced via asymptotic giant branch (AGB) stars. In this paper we explore the side-effects of this model with a view to identifying possible observational signatures other than increased heavy Mg isotope abundances.

The paper is organised as follows. The remainder of this section summarizes the QSO absorption-line evidence for and against variations in  $\alpha$  and describes the sensitivity of that evidence to variations in isotopic abundances. Section 2 briefly describes the nucle-

osynthesis of Mg isotopes in stars of different masses. In Section 3 we detail our chemical evolution models and compare them with those used by AMO04. Section 4 presents our main results for the predicted evolution of the total and isotopic abundances of various elements typically observed in QSO spectra. In each case we compare these with available data from QSO absorption-line and local stellar and interstellar medium (ISM) studies and discuss their dominant uncertainties. Section 5 assesses the overall validity of the IM-enhanced models in light of our new results and presents other arguments for and against such models. Section 6 gives our main conclusions.

### 1.1 Evidence for varying $\alpha$ from QSO absorption systems?

The universality and constancy of the laws of nature rely on the space-time invariance of fundamental constants, such as  $\alpha$ . Therefore, since Milne (1935, 1937) and Dirac (1937) first suggested the time-variation of the Newton gravitational constant, a great diversity of theoretical and experimental exploration of possible space-time variations in fundamental constants has been pursued (e.g. see review in Uzan 2003).

High resolution spectroscopy of absorption systems lying along the lines-of-sight to background QSOs has provided particularly interesting constraints on variations in  $\alpha$  over large spatial and

★ E-mail: yfenner@astro.swin.edu.au, mim@ast.cam.ac.uk

temporal baselines. Early work focused on the alkali-doublet (AD) method: since the relative wavelength separation between the two transitions of an AD is proportional to  $\alpha^2$  (e.g. Bethe & Salpeter 1977), comparison between AD separations seen in absorption systems with those measured in the laboratory provides a simple probe of  $\alpha$  variation. Several authors (e.g. Varshalovich & Potekhin 1994; Cowie & Songaila 1995; Varshalovich, Panchuk & Ivanchik 1996; Varshalovich, Potekhin & Ivanchik 2000) applied the AD method to doublets of several different ionic species (e.g. C IV, Si II, Si IV, Mg II and Al III). The strongest current AD constraints come from analysis of many Si IV absorption systems in  $R \sim 45\,000$  spectra:  $\Delta\alpha/\alpha = (-0.5 \pm 1.3) \times 10^{-5}$  (Murphy et al. 2001c, 21 systems;  $2.0 < z_{\text{abs}} < 3.0$ ) and  $\Delta\alpha/\alpha = (0.15 \pm 0.43) \times 10^{-5}$  (Chand et al. 2004b, 15 systems;  $1.6 < z_{\text{abs}} < 2.9$ )<sup>1</sup>.

Considerable recent interest has focused on the many-multiplet (MM) method introduced by Dzuba, Flambaum & Webb (1999a,b) and Webb et al. (1999). The MM method is a generalization of the AD method, constraining changes in  $\alpha$  by utilizing many observed transitions from different multiplets and different ions associated with each QSO absorption system. It holds many important advantages over the AD method, including an effective order-of-magnitude precision gain stemming from the large differences in sensitivity of light (e.g. Mg, Si, Al) and heavy (e.g. Fe, Zn, Cr) ions to varying  $\alpha$ . At low redshift ( $0.5 \lesssim z_{\text{abs}} \lesssim 1.8$ ), Mg lines, whose red transition wavelengths ( $\lambda > 2700 \text{ \AA}$ ) are relatively insensitive to changes in  $\alpha$ , act as anchors against which the larger expected shifts in the bluer ( $2300 < \lambda < 2700 \text{ \AA}$ ) Fe transition wavelengths can be measured. At higher  $z_{\text{abs}}$ , transitions from Si and Al provide anchor lines distributed in wavelength space amongst a variety of Cr, Fe, Ni and Zn transitions which shift by large amounts in both positive and negative directions as  $\alpha$  varies. This diversity at high- $z_{\text{abs}}$  ensures greater reliability in the face of simple systematic effects compared with the low- $z_{\text{abs}}$  Mg/Fe systems.

The MM method, applied to Keck/HIRES QSO absorption spectra, has yielded very surprising results, with the first tentative evidence for a varying  $\alpha$  by Webb et al. (1999) becoming stronger with successively larger samples (Murphy et al. 2001a; Webb et al. 2001; Murphy, Webb & Flambaum 2003). The most recent Keck/HIRES constraint comes from 143 absorption systems over the range  $0.2 < z_{\text{abs}} < 4.2$  (MFW04):  $\Delta\alpha/\alpha = (-0.57 \pm 0.11) \times 10^{-5}$ . This result is quite internally robust: it comprises three different observational samples and approximately equal low- and high- $z_{\text{abs}}$  subsamples, all of which give consistent results. Stubbornly, it has also proven resistant to a range of potential instrumental and astrophysical systematic effects (Murphy et al. 2001b, 2003).

Intriguingly, Chand et al. (2004a) (see also Srianand et al. 2004) have analysed 23 Mg/Fe absorption systems in higher signal-to-noise ratio (S/N) spectra from a different telescope and spectrograph, the VLT/UVES, claiming a precise, null result over the range  $0.4 < z_{\text{abs}} < 2.3$ :  $\Delta\alpha/\alpha = (-0.06 \pm 0.06) \times 10^{-5}$ . Quast, Reimers & Levshakov (2004) and Levshakov et al. (2004) also find null results in individual UVES absorbers. The discrepancy between the VLT/UVES and Keck/HIRES results is yet to be resolved. However, it is important to note that low-order distortions of the Keck/HIRES wavelength scale, as might be expected from simple instrumental systematic errors, produce opposite effects on the low- and high- $z_{\text{abs}}$  samples and so cannot fully explain the HIRES-UVES difference (Murphy et al. 2003, 2004). If

the HIRES result is incorrect, the nature of the contributory systematic errors must be subtle and somewhat conspiratorial.

## 1.2 Isotopic abundance evolution?

Murphy et al. (2001b) first identified the potential systematic error introduced into the MM method if the relative isotopic abundances of crucial anchor elements like Mg and Si underwent strong cosmological evolution. This is because the absorption lines of the different isotopes are spaced widely enough ( $\sim 0.5 \text{ km s}^{-1}$ ) in these light ions to affect the measured line centroids (Fig. 1, left panel). MFW04 calculated  $\Delta\alpha/\alpha$  from their HIRES absorption line data as a function of the assumed relative isotopic abundances of Mg and Si. The results are presented in the right panel of Fig. 1. Note the relative insensitivity of  $\Delta\alpha/\alpha$  in the high- $z_{\text{abs}}$  systems to the Si heavy isotope ratio,  $(^{29}\text{Si} + ^{30}\text{Si})/^{28}\text{Si}$ . As noted above, this is expected because of the greater diversity of transitions and line-shifts available in the high- $z_{\text{abs}}$  regime. It is therefore important to note that evolution in the Si isotopic abundance cannot explain the high- $z_{\text{abs}}$  HIRES results. Until recently, no information about the isotopic shifts in transitions from heavier ions used at high- $z_{\text{abs}}$  (e.g. Cr II, Fe II, Ni II, Zn II) were available. However, due to their higher masses, the shifts are expected to be smaller with respect to the sensitivity of the lines to varying  $\alpha$ . Indeed, the recent isotopic shift calculations of Kozlov et al. (2004) confirm this.

However, Fig. 1 emphasises the strong dependence of  $\Delta\alpha/\alpha$  in the low- $z_{\text{abs}}$  systems on the Mg heavy isotope ratio,  $(^{25}\text{Mg} + ^{26}\text{Mg})/^{24}\text{Mg}$ . The importance of this potential systematic effect therefore depends entirely on the evolution of Mg isotopic ratios in QSO absorption systems. Unfortunately, no direct measurement of  $(^{25}\text{Mg} + ^{26}\text{Mg})/^{24}\text{Mg}$  in QSO absorbers is currently feasible due to the small separation of the isotopic absorption lines. Fortunately however, Mg is one of the few elements for which stellar isotopic abundances can be measured through molecular absorption lines, in this case transitions of MgH. Gay & Lambert (2000) and Yong, Lambert & Ivans (2003b) have shown that observed stellar values of  $(^{25}\text{Mg} + ^{26}\text{Mg})/^{24}\text{Mg}$  generally decrease with decreasing [Fe/H], as predicted in the Galactic chemical evolution models of Timmes, Woosley & Weaver (1995). The (normal IMF) model we present in Section 3 also predicts such a decrease (Fig. 2). This has been used to argue that in the low-metallicity environments of Mg/Fe absorbers (typically,  $[\text{Zn}/\text{H}] \sim -1.0$ ), one should expect sub-solar values of  $(^{25}\text{Mg} + ^{26}\text{Mg})/^{24}\text{Mg}$  and so, if anything, one expects the low- $z_{\text{abs}}$  values of  $\Delta\alpha/\alpha$  to be *too positive* (Murphy et al. 2001b, 2003, 2004; Chand et al. 2004a).

Contrary to this trend, Yong et al. (2003a) have found very high values of  $(^{25}\text{Mg} + ^{26}\text{Mg})/^{24}\text{Mg}$  for some giant stars in the globular cluster NGC 6752, which has metallicity  $[\text{Fe}/\text{H}] \sim -1.6$ . One star had  $(^{25}\text{Mg} + ^{26}\text{Mg})/^{24}\text{Mg} = 0.91$  (cf.  $(^{25}\text{Mg} + ^{26}\text{Mg})/^{24}\text{Mg}_{\odot} = 0.27$ ). Since IM AGB stars are thought to produce significant quantities of  $^{25}\text{Mg}$  and  $^{26}\text{Mg}$  (see Section 2), Yong et al. (2003a) proposed that low-metallicity, IM AGB stars may have polluted this globular cluster. This prompted Ashenfelter et al. (2004a,b) to propose a chemical evolution model with a strongly enhanced population of IM stars as a possible explanation for the low- $z_{\text{abs}}$  HIRES varying- $\alpha$  results. In the following sections we describe in detail the nucleosynthesis of Mg isotopes and construct a chemical evolution model, similar to that of AM04, to investigate the various effects of an IM-enhanced IMF.

<sup>1</sup>  $\Delta\alpha/\alpha$  is defined as  $\Delta\alpha/\alpha = (\alpha_z - \alpha_0)/\alpha_0$ , for  $\alpha_z$  and  $\alpha_0$  the values of  $\alpha$  in the absorption system(s) and in the laboratory respectively.

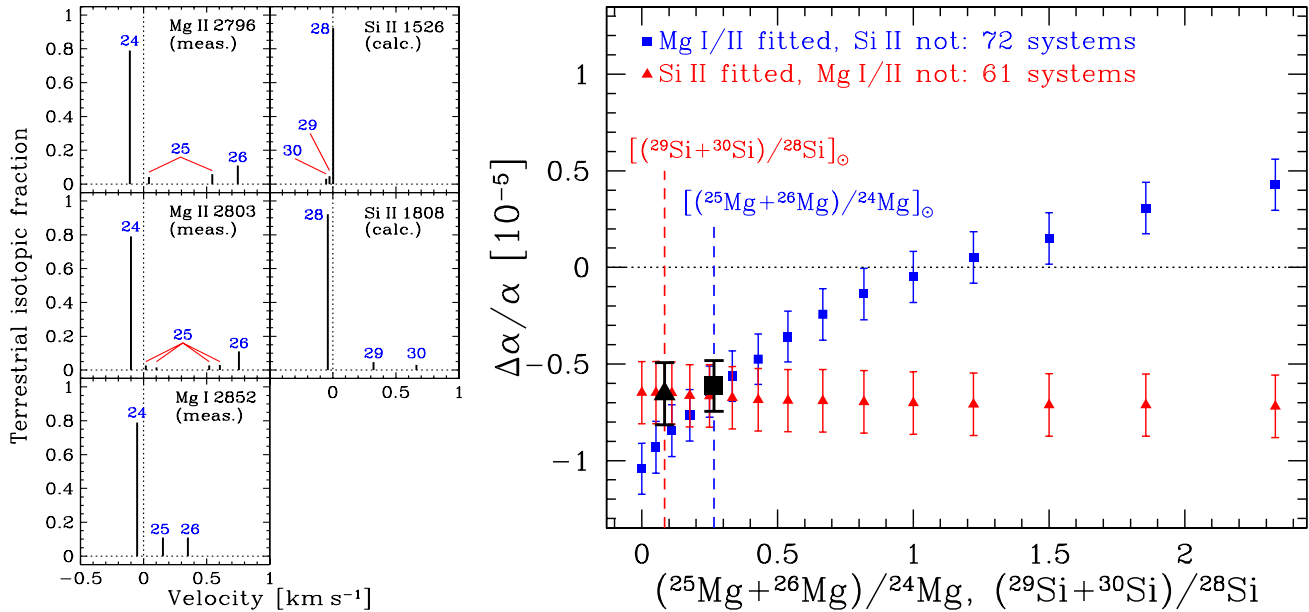


**Figure 1.** Left panel: Isotopic structures for the relevant Mg/Si transitions from measurements (Hallstadius 1979; Drullinger et al. 1980; Pickering et al. 1998) or calculations (Berengut et al. 2003). Zero velocity corresponds to the isotopic structure's centre of gravity. Right panel: Sensitivity of  $\Delta\alpha/\alpha$  measured by MFW04 to variations in Mg and Si isotopic abundance variations. Absorption systems containing no measured Si lines (i.e. most low- $z_{\text{abs}}$  systems) contribute to the square points while only systems containing Si lines and no measured Mg lines (i.e. most high- $z_{\text{abs}}$  systems) contribute to the triangular points. The large square and triangle mark the values of  $\Delta\alpha/\alpha$  obtained with terrestrial relative isotopic abundances (Rosman & Taylor 1998):  $(^{24}\text{Mg} : ^{25}\text{Mg} : ^{26}\text{Mg})_{\odot} = (79 : 10 : 11)$  and  $(^{28}\text{Si} : ^{29}\text{Si} : ^{30}\text{Si})_{\odot} = (92.2 : 4.7 : 3.1)$ . The abundance ratio of the heavy isotopes [i.e.  $(^{25}\text{Mg} : ^{26}\text{Mg})$  and  $(^{29}\text{Si} : ^{30}\text{Si})$ ] was held at the terrestrial value along the abscissa.

## 2 NUCLEOSYNTHESIS OF MAGNESIUM ISOTOPES

Massive stars culminating in Type II SNe are responsible for most of the Mg isotopes in the present-day Galaxy. However, there is evidence that intermediate-mass stars may dominate the production of the neutron-rich Mg isotopes in the metal-poor regime. According to standard models of stellar nucleosynthesis, the yield of the heavy Mg isotopes,  $^{25,26}\text{Mg}$ , scales with the initial stellar metallicity. Conversely, the generation of  $^{24}\text{Mg}$  from SNe II operates fairly independently of initial metallicity. Since massive stars alone are insufficient to account for the higher than expected values of  $^{25,26}\text{Mg}/^{24}\text{Mg}$  detected in metal-poor stars (Gay & Lambert 2000; Yong et al. 2003b), it has been suggested that there is a supplemental source of the neutron-rich Mg isotopes.

Karakas & Lattanzio (2003) have shown that  $^{25}\text{Mg}$  and  $^{26}\text{Mg}$  production is substantial in metal-poor intermediate-mass stars (IMSSs). At low metallicities, asymptotic giant branch stars are believed to generate  $^{25}\text{Mg}$  and  $^{26}\text{Mg}$  from  $\alpha$ -capture onto  $^{22}\text{Ne}$  triggered by He-shell thermal pulsing. Temperatures at the base of the convective envelope in 4–6  $\text{M}_{\odot}$  stars can be high enough to burn  $^{24}\text{Mg}$  via hot bottom burning (HBB) as well as synthesise large amounts of  $^{25}\text{Mg}$  and  $^{26}\text{Mg}$ . Based on the recent nucleosynthetic calculations from Karakas & Lattanzio (2003), AGB stars have been shown to produce sufficient quantities of  $^{25,26}\text{Mg}$  to resolve the discrepancy between local stellar observations and previous model predictions (Fenner et al. 2003). For the present study, we have incorporated the same grids of low- and intermediate-mass stellar yields that successfully reproduced the solar neighbourhood Mg isotopic evolution.

## 3 CHEMICAL EVOLUTION MODELS

The distribution of elements and isotopes as a function of time and radius was simulated for a Milky Way-like disk galaxy by numerically solving the classic set of equations (as described by Tinsley 1980) governing gas infall, star formation, stellar evolution and nucleosynthesis. In particular, we present predictions for (i) the solar annulus ( $r = 8.5$  kpc) because it is the solar neighbourhood for which we have the most comprehensive set of empirical constraints, and (ii) the outer disk ( $r = 16.5$  kpc) because it is possible that many QSO absorption systems correspond to the outer regions of spiral disks (e.g. Dessauges-Zavadsky et al. 2004). To summarise the details of the model: we define  $\sigma_i(r, t)$  as the mass surface density of species  $i$  at time  $t$  and radius  $r$ , and assume that its rate of change of is given by:

$$\frac{d}{dt}\sigma_i(r, t) = \int_{m_{\text{low}}}^{m_{\text{up}}} \psi(r, t - \tau_m) Y_i(m, Z(r, t - \tau_m)) \frac{\phi(m)}{m} dm + \frac{d}{dt}\sigma_i(r, t)_{\text{infall}} - X_i(r, t) \psi(r, t), \quad (1)$$

where the three terms on the right-hand side correspond to the stellar ejecta, gas infall, and star formation, respectively. The star formation rate,  $\psi$ , varies with the square of the gas surface density in our models, consistent with the empirical Schmidt (1959) law.  $Y_i(m, Z(r, t - \tau_m))$  denotes the stellar yield of  $i$  (in mass units) from a star of mass  $m$  and metallicity  $Z(r, t - \tau_m)$ ,  $\phi(m)$  is the initial mass function, and  $X_i$  is the mass fraction of element  $i$ . By definition, the sum of  $X_i$  over all  $i$  is unity. The total surface mass density is identical to the integral over the infall rate. The lower and upper stellar mass limits,  $m_{\text{low}}$  and  $m_{\text{up}}$ , are 0.08  $\text{M}_{\odot}$  and 60  $\text{M}_{\odot}$ , respectively, while  $\tau_m$  is the main-sequence lifetime of a star of mass  $m$ . We split the first term into three equations that deal separately with low- and

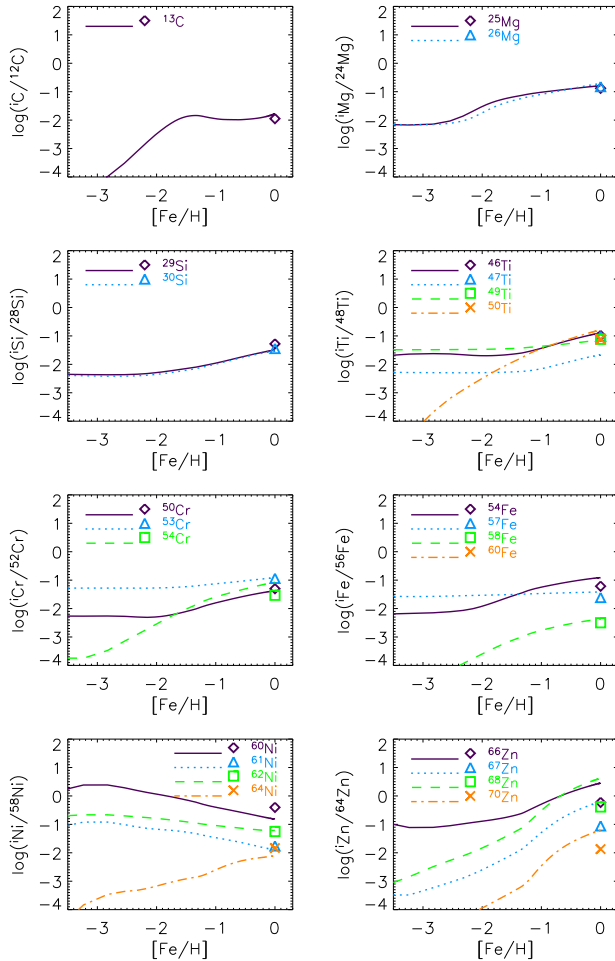


**Figure 2.** The evolution of isotopic ratios with metallicity  $[Fe/H]$  for the elements C, Mg, Si, Ti, Cr, Fe, Ni, Zn, which are used in varying  $\Delta\alpha/\alpha$  analyses. Isotopic abundances are shown on a logarithmic scale relative to the dominant isotope for that element. Different curves illustrate the predicted behaviour of the various isotopes from a standard solar radius chemical evolution model. Symbols show the corresponding solar values. In general, the minor isotopes accrue more slowly in the ISM with respect to the dominant isotope for each element. A notable exception is Ni, for which  $^{60,62}\text{Ni}/^{58}\text{Ni}$  declines over time. The departure of Ni from the general rule of thumb may reflect uncertainties in its nucleosynthesis, including an overproduction from SNe Ia, that have been pointed out in the literature (e.g. Timmes et al. 1995; Iwamoto et al. 1999).

intermediate-mass stars, Type Ia supernova (SN) progenitors, and massive stars.

Further details of the numerical code employed in this study can be found in Fenner & Gibson (2003), Fenner et al. (2003) and Fenner, Prochaska & Gibson (2004).

### 3.1 Infall scheme

We assumed that the Milky Way-like disk galaxy formed during two main gas accretion episodes. The first occurs on a rapid timescale ( $< 0.5$  Gyr) and is associated with the formation of the halo and thick disk, while the second episode occurs on a longer timescale and fuels the formation of stars in the disk. For simplicity, we have assumed no prior metal-enrichment of the gas infalling onto the disk, although there is some evidence from observations

of high-velocity clouds that gas falling into the Galaxy may contain traces of heavy elements (e.g. Wakker et al. 1999; Gibson et al. 2001; Sembach et al. 2002). Exponentially decaying infall rates have been adopted, such that the evolution of total surface mass  $\sigma_{\text{tot}}(r, t)$  density is given by

$$\frac{d\sigma_{\text{tot}}(r, t)}{dt} = A(r)e^{-t/\tau_H(r)} + B(r)e^{-(t-t_{\text{delay}})/\tau_D(r)} \quad (2)$$

where the infall rate coefficients  $A(r)$  and  $B(r)$  are chosen in order to reproduce the present-day surface mass density of the halo/thick disk and thin disk components, which we take to be 10 and  $45 \text{ M}_\odot \text{ pc}^{-2}$ , respectively. The adopted timescales for the infall phases are  $\tau_H = 0.1$  Gyr and  $\tau_D = 9.0$  Gyr at the solar radius  $r_\odot = 8.5$  kpc. Disk formation starts after an initial delay  $t_{\text{delay}} = 0.5$  Gyr. The ‘inside-out’ functional form for  $\tau_D(r)$  (Romano et al. 2000) is adopted, whereby the timescale for disk gas accretion increases linearly with radius. The Milky Way age is taken to be 13 Gyr.

### 3.2 Initial mass function (IMF)

The shape of the stellar initial mass function (IMF) influences the quantity of Galactic material locked up in stars of different masses, which in turn determines the rate at which different elements are released into the ISM. The models presented in Section 4 compare the Kroupa, Tout & Gilmore (1993) three-component IMF with one enhanced in AGB stars at low metallicities. The shape of the IM-enhanced IMF at time  $t = 0$  is illustrated in Fig. 3. The height and width of the AGB bump was chosen to approximate that in AMO04. It is centred on  $5 \text{ M}_\odot$  with a narrow mass range, although not as narrow as the AMO04 Model 1, for which the extra AGB population consists almost entirely of  $5\pm1 \text{ M}_\odot$  stars (compare our Fig. 3 with their figure 3). Their preferred models (i.e. Models 2 and 3) adopt a wider IM-bump and we also favour a broader peak, on the grounds that it is more physically realistic<sup>2</sup>.

In our IM-enhanced models, the amplitude of the IM-bump decays exponentially with increasing gas metallicity. This differs from AMO04, who adopted time-dependent decay. Imposing a metallicity- rather than time-dependent IM-enhancement was designed to reflect the different physical properties of metal-poor gas clouds. The decreased cooling rate and magnetic field strength in metal-poor material is expected to influence the mass distribution of newly formed stars. For consistency with AMO04 Model 1, our scale-factor for the exponentially decaying IM-bump was chosen to correspond to the predicted metallicity at the solar radius at time = 0.2 Gyr. This corresponds to  $[Z/H] \sim -1.3$ , or roughly 1/20th solar metallicity. The transformation from a time- to a metallicity-dependent IMS burst makes it reasonable to apply the same IMF formalism across all Galactic radii. Because the outer disk has a more protracted star formation rate and builds up metals more slowly than in the solar radius, the effects of an IMS burst would be suppressed by adopting a fixed timescale. Instead, conversion to metallicity-dependence prolongs the temporal duration of the IMS burst at outer radii and amplifies the chemical signature of an IM-enhanced IMF.

<sup>2</sup> As a check, we ran a model using a narrower and taller IM-bump, conserving the mass contained in the AGB-enhancement. The final results were similar in both cases.

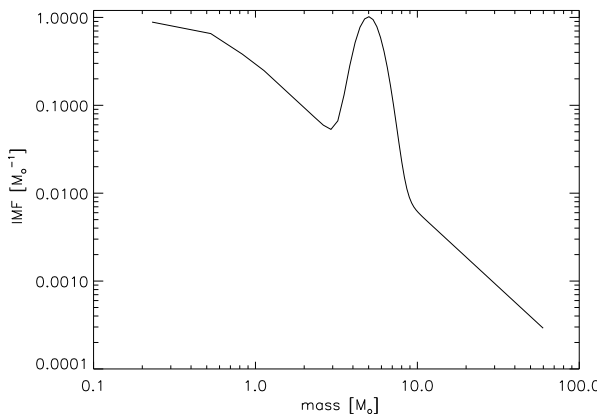


**Figure 3.** The shape of the IM-enhanced IMF used in this study at time  $t = 0$ . The IMF is composed of an AGB-biased bump superimposed on a standard Kroupa, Tout & Gilmore (1993) 3-component power-law. The height and width of the AGB bump was chosen to emulate that in AMO04. The amplitude of the bump decays exponentially with increasing gas metallicity.

### 3.3 Stellar Yields and Lifetimes

*Low and intermediate mass stars (LIMS):* For stars less massive than  $8 M_\odot$ , we incorporated the yields from the stellar evolution and nucleosynthesis code described in Karakas & Lattanzio (2003), supplemented with yields for additional isotopes from hydrogen to sulfur and for the iron-peak, as well as unpublished yields for the metallicity  $Z=0.0001$ . The wide range of heavy elements and isotopes incorporated in these AGB nucleosynthesis models allows us to self-consistently predict the contribution from low- and intermediate-mass stars (LIMS) to the elemental and isotopic abundance of many species of interest in DLA and varying  $\alpha$  studies. These include C, N, Mg, Al, Si, Ni and Fe. We also ran identical chemical evolution models using two alternative sets of LIMS yields: those of (i) van den Hoek & Groenewegen (1997) and (ii) Marigo (2001) (using mixing length parameter  $\alpha = 2$  for consistency with AMO04). These two alternative inputs do not predict yields for elements beyond O, but they provide an indication of the uncertainty in the CNO yields, as will be discussed in Section 4.6.

*Type Ia supernovae (SNe Ia):* We adopted a recalculation of the Thielemann, Nomoto, & Yokoi (1986) W7 model by Iwamoto et al. (1999) to estimate the yields from SNe Ia. It was assumed that 4% of binary systems involving intermediate and low mass stars result in SNe Ia, since this fraction provides a good fit to the solar neighbourhood (e.g. Alibés, Labay, & Canal 2001; Fenner & Gibson 2003).

*Massive stars:* For stars more massive than  $8-10 M_\odot$  that end their lives in violent supernova explosions, we implemented the yields from Woosley & Weaver (1995). Their yields span metallicities from zero to solar and cover the mass range  $11-40 M_\odot$ . Since the upper mass limit of our stellar IMF extends beyond this mass range, we extrapolated the  $35$  and  $40 M_\odot$  yields for  $m > 40 M_\odot$ . We took the lower energy ‘A’ models for stars  $\leq 25 M_\odot$  and the higher energy ‘B’ models for heavier stars. Taking note of the suggestion by Timmes, Woosley, & Weaver (1995) that the WW95 mass-cuts may have penetrated too deeply within the iron core, we have uniformly halved the iron yields from these models. In the uncertain mass range  $8-12 M_\odot$ , we make the conservative assumption that these stars do not synthesise new heavy elements, but expel mate-

rial with the same heavy element abundance pattern as the gas from which they were born.

*Stellar lifetimes:* We adopt metallicity-dependent main-sequence lifetimes calculated by Schaller et al. (1992). Although stars lose material over the course of their evolution via stellar winds and planetary nebulae, this model assumes that all the mass loss takes place at the end of the main-sequence phase. Our predictions are not significantly affected by this simplification.

### 3.4 Comparison with Ashenfelter et al. (2004)

We now list some key differences between our model and that of Ashenfelter et al. (2004b) and describe the impact on the results:

- **AGB yields:** We have adopted the low- and intermediate-mass stellar yields from Karakas & Lattanzio (2003), with additional yields for isotopes up to S as well as the Fe-peak, along with unpublished yields for the metallicity  $Z=0.0001$ . Thus, the AGB yields of species such as N and the Mg isotopes are internally self-consistent. AMO04 added the Mg isotopic yields from Karakas & Lattanzio (2003) onto the Marigo (2001) C, N and O yields. Although this means that their N yields were not drawn from the same AGB models as the Mg yields, the predicted evolution of N is very similar in either case, as discussed in Section 4.6.2.

- **Type Ia SNe yields:** AMO04 employed a metallicity-dependent Type Ia supernovae rate from Kobayashi, Tsujimoto & Nomoto (2000) that prohibits the formation of SNe Ia below a minimum [Fe/H] threshold of  $-1.1$ . This metallicity-dependence was postulated mostly on theoretical grounds. Observationally however,  $\alpha/\text{Fe}$  ratios in dwarf galaxies (e.g. Shetrone et al. 2001) and S/Zn ratios in DLAs (Pettini, Ellison, Steidel & Bowen 1999) provide evidence for SN Ia activity below  $[\text{Fe}/\text{H}] \sim -1$ . Furthermore, the trend of  $[\text{O}/\text{Fe}]$  with  $[\text{Fe}/\text{H}]$  seen in local stars can be satisfactorily explained without imposing a SN Ia metallicity threshold (e.g. Alibés et al. 2001). Thus, the present study does not impose a metallicity threshold and the SN Ia rate is calculated following the method of Gregg & Renzini (1983) and Matteucci & Gregg (1986). While a  $[\text{Fe}/\text{H}] \sim -1$  SN Ia threshold would have only a minor effect on the solar radius results, the outer disk remains metal-poor for at least several Gyr and would be more sensitive to the precise SN Ia prescription, as will be discussed in Section 4.

- **Standard IMF:** In recalculating the model of Timmes et al. (1995), AMO04 adopted the Salpeter (1955) single power-law IMF. We adopt a three-component Kroupa et al. (1993) law, which is flatter at lower masses and steeper at the high end of the IMF. This empirically derived function leads to a lower overall effective yield that is more consistent with local data (Pagel 2001). Although the choice of IMF does influence the evolution of the chemical species of interest in this investigation, the impact is not large enough to affect our final conclusions. Model 1 from AMO04 also differs from our IM-enhanced model through the inclusion of an exponential 0.5 Gyr time scale before the onset of the “normal” stellar IMF component. Thus, at the very earliest times, most of the star-forming gas ends up inside stars with  $m \sim 5 M_\odot$ . In contrast, we retain our normal IMF component at all times (akin to AMO04’s Model 2).

- **IM-enhanced IMF:** While the AMO04 IM-bump decays exponentially on a fixed timescale (ranging from 0.2 to 0.4 Gyr depending on the model), we transformed this from a time to a metallicity dependence. As discussed in Section 3.2, the assumption that the shape of the IMF is governed primarily by the chemical composition of the star forming gas cloud is presumably more physically justified than imposing a uniform time-dependence. Convert-

ing from the time to the metallicity domain allows us to apply the same IMF prescription to systems with various star formation histories, such as the slowly evolving outer Galactic disk, which we investigate in this paper.

- **Dual-phase infall:** AMO04 assumed that the Galactic disk forms during a *single* phase of gas infall, in order to directly compare with the results of Timmes et al. (1995). We model the Milky Way formation using a *dual*-phase infall scheme, since this has been shown to provide a better match than single-infall models to the number distribution of G- and K-dwarfs in the solar neighbourhood (e.g. Chiappini et al. 1997). We stress that our final conclusions are largely insensitive to our choice of infall scheme.

## 4 RESULTS

We now present the predicted chemical evolution for the solar radius and the outer Galactic disk in the case of an enhanced population of intermediate-mass stars at low metallicity. These results are compared with those obtained using a normal IMF and plotted against observations of local stars and DLAs, where applicable. In all the following figures, solid and dashed lines denote the evolution at the solar (8.5 kpc) and outer radii (16.5 kpc), respectively. Models adopting a normal IMF are shown with thin lines, while thick lines correspond to models with the IM-enhanced IMF, as illustrated in Fig. 3.

### 4.1 Type Ia supernova rate and the age-metallicity relationship

The evolution of the Type Ia supernova rate predicted by the model described in Section 3 is shown in the upper panel of Fig. 4. The incidence of Type Ia SNe in the solar region (solid lines) is predicted to have risen to a peak about 7 Gyr ago and steadily declined thereafter. In contrast, the predicted SN Ia rate in the outer disk (dashed lines) has continued to increase up to the present-day. This difference reflects the more rapid and efficient conversion of gas into stars in regions of higher surface density.

A consequence of an IMF that increases the number of intermediate-mass stars is the birth of more Type Ia SNe progenitors. Type Ia SNe are understood to be associated with binary systems of low- and intermediate-mass stars, in which the mass lost by the more evolved star is accreted by its white dwarf (WD) companion until the WD can no longer be sustained by electron degenerate pressure and a violent explosion ensues. Comparing the thick and thin solid lines in the upper panel of Fig. 4, it can be seen that the IM-enhanced IMF has no significant affect on the local solar neighbourhood SN Ia rate. In the outer disk, however, the AGB-enhancement elevates the SN Ia rate by up to a factor of six between 0.5–1 Gyr and about a factor two at 3 Gyr before converging with the normal IMF model after  $\sim$ 6 Gyr (compare the thick and thin dashed lines). The different impact of the IM-enhanced IMF on the solar and outer radii is due to a faster build-up of metals in the solar radius relative to the outer disk. This causes the IM-bump to decay more quickly and leads to only a minor increase in the SN Ia rate. In contrast, the slower rate of enrichment in the outer radius leads to a longer-lasting IM-bump, which has a significant impact on the SN Ia rate at early times. IM-enhanced IMFs at low metallicity could leave an observable trace on the cosmic SN Ia rate, which could be used to discriminate between these models (Fields et al. 2001).

Type Ia SNe are major producers of iron and are responsible

for 1/3–2/3 of the solar Fe content (e.g. Timmes et al. 1995). Thus, any increased incidence of SN Ia leads inevitably to the production of more Fe, as seen in the lower panel of Fig. 4 where the evolution of [Fe/H] is plotted. The inclusion of an enhanced IM AGB population increases the abundance of iron in the ISM of the outer disk by a factor of 2–3 between 1–3 Gyr. Once again, the solar radius is less sensitive to the IM-enhanced IMF because the amplitude of the IM-bump decays on a shorter timescale.

As well as being SN Ia progenitors, AGBs leave behind white dwarf remnants that can be indirectly detected through microlensing experiments. We found that the IM-enhanced IMF increases the present-day number of WD remnants by only about 5% and 10% for the solar and outer radii, respectively. Thus, the number of WDs is not expected to be a sensitive discriminant of the different IMF scenarios. This echos the Galactic halo results of Gibson & Mould (1997) and Fields, Freese, & Graff (2000), who found that stellar C and N abundances provide far stronger constraints than WD counts on any enhancement in the number of LIMS at early times.

It should be noted that although AMO04 only predict the evolution at the solar radius, if their IM-enhanced model were applied to the outer disk we expect that they would *not* predict an increase in either the SN Ia rate or [Fe/H] because their SN Ia prescription prohibits the formation of Type Ia SNe in metal-poor environments.

### 4.2 Magnesium isotopic ratio

Figure 5 shows the sensitivity of  $(^{25}\text{Mg} + ^{26}\text{Mg})/^{24}\text{Mg}$  versus [Fe/H] to the choice of IMF for both the solar (8.5 kpc) and outer (16.5 kpc) radius models. Predictions are plotted against abundances observed in nearby dwarf stars by Gay & Lambert (2000; circles) and Yong et al. (2003b; diamonds). It has been suggested that the production of heavy Mg isotopes by IMSs is needed to explain the observations in metal-poor stars (e.g. Timmes et al. 1995; Goswami & Prantzos 2000; Alibés et al. 2001). Indeed, Fenner et al. (2003) found that IMSs were responsible for most of the heavy Mg isotopes in the solar neighbourhood for  $[\text{Fe}/\text{H}] < -1$ . The inclusion of AGB nucleosynthesis within the framework of the standard IMF model provides a good match to both datasets at low [Fe/H], as illustrated by the thin solid line in Fig. 5. At higher [Fe/H], the normal IMF solar model matches the Gay & Lambert (2000) data but not those of Yong et al. (2003b). We caution that our predictions are best compared against the Gay & Lambert (2000) sample because Yong et al. (2003b) used kinematics to preferentially select halo and thick disk stars. Consequently, their sample contains relatively few thin disk members and perhaps some stars belonging to an accreted component (although inspection of figure 13 from Yong et al. 2003 indicates that the fraction of accreted stars is small if one employs the Gratton et al. 2003 criteria to specify the accreted component). An uncertainty in the  $^{25}\text{Mg}$  and  $^{26}\text{Mg}$  yields of  $\pm 0.2$  dex is illustrated for the IM-enhanced solar radius model by the shaded region in Fig. 5, and will be discussed further in Section 4.6.1.

Although the mean  $(^{25}\text{Mg} + ^{26}\text{Mg})/^{24}\text{Mg}$  for all stars with  $[\text{Fe}/\text{H}] < -1$  is about 0.15, Fig. 1 demonstrates that a value 5–9 times larger than this is required to explain the  $\Delta\alpha/\alpha$  measured by MFW04, under the assumption of a solar  $^{25}\text{Mg} : ^{26}\text{Mg}$  ratio. AMO04 estimated that a ratio of  $(^{25}\text{Mg} + ^{26}\text{Mg})/^{24}\text{Mg} = 0.62$  would remove the need for any time-variation in  $\alpha$ . This is lower than our calculated value of  $1.1 \pm 0.3$  (see Fig. 1) because theirs is only a rough approximation and ours is based on the QSO absorption-line spectra. However, to aid comparison, we followed AMO04 in imposing an IM-enhanced IMF capable of elevating

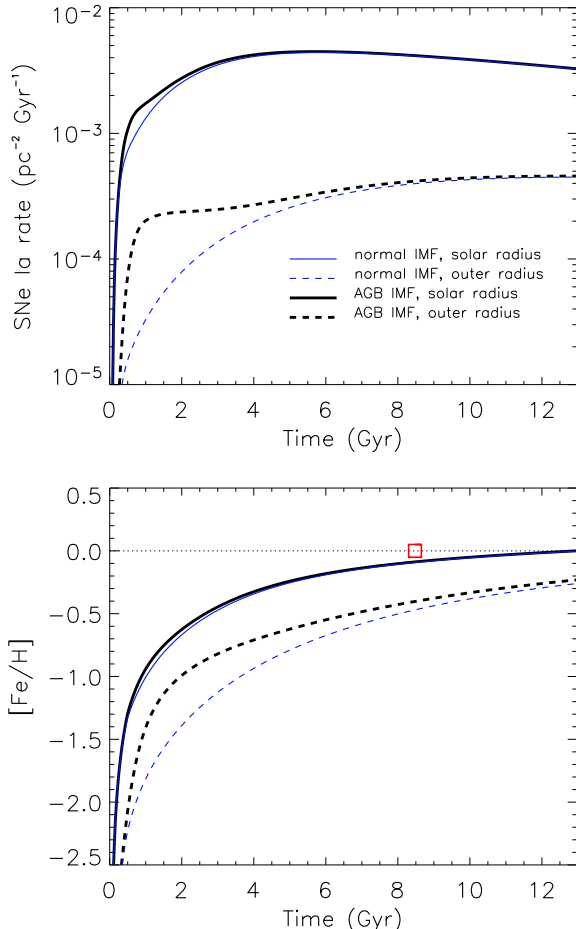


**Figure 4.** *Upper panel:* Type Ia supernovae rate as a function of time for the solar neighbourhood (solid lines) and the outer disk (dashed lines) in the case of a normal IMF (thin lines) versus the IM-enhanced IMF (thick lines). *Lower panel:* Trend of [Fe/H] vs time. The square shows the position of the sun, while lines have the same meaning as in the panel above. Due to a faster build-up of metals in the solar radius relative to the outer disk, the IM-bump decays more quickly and leads to only a minor increase in the SN Ia rate and, consequently, the [Fe/H] evolution. In contrast, the slower rate of enrichment in the outer radius leads to a longer-lasting IM-bump, which has a significant impact on the SN Ia rate and Fe content at early times.

$(^{25}\text{Mg}+^{26}\text{Mg})/^{24}\text{Mg}$  to  $\sim 0.62$  for the solar radius model (thick solid line).

The behaviour of the Mg isotopic ratios in our IM-enhanced solar radius model is very similar to AM004 Model 1, reaching a maximum of  $(^{25}\text{Mg}+^{26}\text{Mg})/^{24}\text{Mg} = 0.63$  at  $[\text{Fe}/\text{H}] = -1.65$ . The prolonged impact of the IM-enhanced IMF in the more metal-poor outer disk leads to a maximum  $(^{25}\text{Mg}+^{26}\text{Mg})/^{24}\text{Mg}$  ratio of 0.92 at  $[\text{Fe}/\text{H}] = -1.7$ . This is seven times higher than the corresponding ratio in the case of the normal IMF. If we assume that (i) the level of AGB stellar enhancement is a function of gas metallicity and declines with the build-up of metals, and (ii) that many QSO absorption systems consist of slowly evolving objects such as dwarfs or outer disks of spirals, then these findings are qualitatively consistent with a scenario in which much higher neutron-rich Mg isotopic abundances are found in QSO absorption systems than in local stars of the same metallicity.

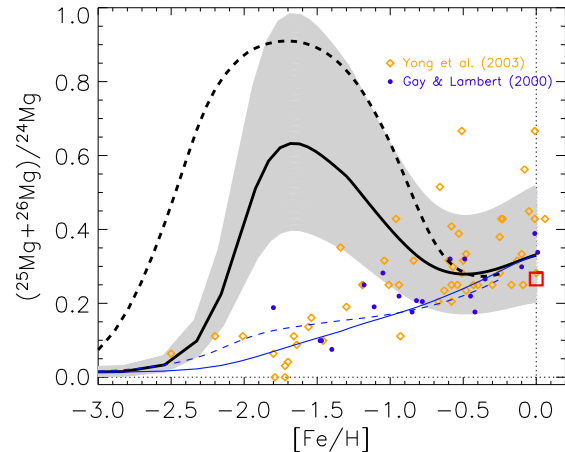


**Figure 5.** Evolution of  $(^{25}\text{Mg}+^{26}\text{Mg})/^{24}\text{Mg}$  as a function of  $[\text{Fe}/\text{H}]$ . As for Fig 4, the solid and dashed lines show predictions for the solar radius and outer disk, respectively. Thin lines denote a normal IMF model and thick lines represent the model with an IM-enhanced IMF. Circles and diamonds show stellar data from Gay & Lambert (2000) and Yong et al. (2003b), respectively. The square shows the solar value. The shaded area indicates a  $\pm 0.2$  dex uncertainty range for the thick solid line.

#### 4.3 Nitrogen

The types of AGB stars responsible for expelling enough heavy Mg isotopes at early times to explain an apparent variation in  $\alpha$  are also thought to be the main factories of primary nitrogen. Thus, an enhanced AGB population should leave a strong imprint on the N abundances in local stars and in DLAs. The predicted variation of  $[\text{N}/\alpha]$  with  $[\alpha/\text{H}]$  is plotted against DLA measurements in Fig. 6. The model results are plotted using Si as the reference element, while for the Centurión et al. (2003) data, the  $\alpha$ -element is O, Si or S. It is reassuring that the normal IMF solar model (thin solid line) passes through the DLA data before rising to roughly solar value. However, no single homogeneous chemical evolution model will account for the broad spread in the DLA data and, worryingly, the outer disk normal IMF model (thin dashed line) overproduces N with respect to the data. Since the normal IMF models (thin lines) already tend to produce more N than is observed in DLAs, it is not surprising that the IM-enhanced IMF models (thick lines) overproduce N by more than an order of magnitude. An indication of the sensitivity of these results to the stellar nucleosynthesis models is given by comparing the thick solid line with the thin dotted line, which corresponds to the IM-enhanced solar radius model in the case of van den Hoek & Groenewegen (1997) IMS yields. Section 4.6.2 describes the uncertainties in these predictions in greater detail.

Inspection of Figs. 5 & 6 reveals that the empirical constraints imposed by DLA nitrogen abundances are strongly violated by the models capable of producing sufficient  $^{25,26}\text{Mg}$  relative to  $^{24}\text{Mg}$  to mimic the variation in the  $\alpha$  obtained by MFW04. AM004 encountered the same problem with their Model 1, which they sought to rectify in Model 2 by increasing star formation efficiency (SFE) by a factor of  $\sim 2.5$ . Figure 7 shows how our  $[\text{N}/\alpha]$  versus  $[\alpha/\text{H}]$  varies with a factor of 2.5 increase in SFE. The agreement with the data is improved, but  $[\text{N}/\alpha]$  is still too high, except at the lowest metallicities.

The curve corresponding to our increased SFE model in Fig. 7 is extremely similar to the dot dash line in figure 15 from AM04.

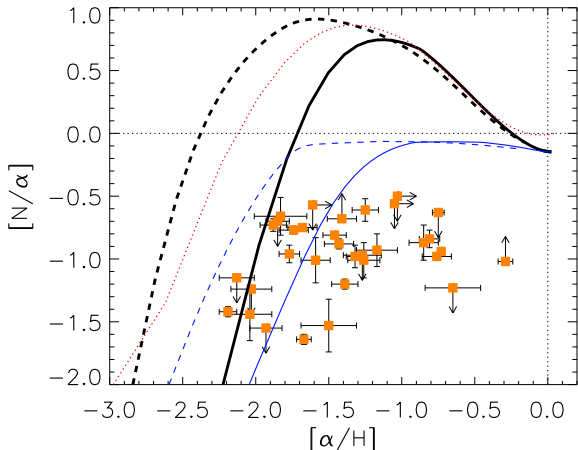


**Figure 6.** Evolution of  $[N/\alpha]$  as a function of  $[\alpha/H]$ . Dashed and solid lines have the same meaning as in Fig 4. Model results employ Si as the reference  $\alpha$ -element. Data points with limits and error bars show DLA measurements by Centurión et al. (2003), where the  $\alpha$ -element is either O, Si, or S. The thin dotted line shows the IM-enhanced solar radius model in the case of van den Hoek & Groenewegen (1997) IMS yields rather than Karakas & Lattanzio (2003), to give an indication of the uncertainties associated with N production in the stellar models.

We note that their Models 1 and 2 differ not just in SFE, but in the location, width, amplitude, and decay timescale of the IMF IM-bump. Nevertheless, we wish to point out a troublesome consequence of such an increase in SFE that is robust to those differences. Figure 8 shows the present-day gas surface density profile expected in the case of normal or enhanced SFE. The standard model agrees with the data from Dame (1993) to within a factor of two. However, a factor of 2.5 increase in the SFE leads to severe gas depletion, in conflict with the observations. While the chemical evolution model that applies to QSO absorption systems need not satisfy the empirical constraints from the Milky Way, we caution that increasing star formation efficiency in order to alleviate overproduction of N might not be appropriate given the gas-rich nature of many absorption systems.

#### 4.4 $^{13}\text{C}/^{12}\text{C}$ abundance ratio

Along with any significant contribution to the abundance of N and the heavy Mg isotopes in metal-poor environments, low- and intermediate-mass stars should leave an additional observable chemical signature in the form of high  $^{13}\text{C}$  abundance relative to  $^{12}\text{C}$ . Metal-poor AGB stars with mass  $\sim 4 M_\odot$  are a major source of  $^{13}\text{C}$ , produced during hot bottom burning when the CN cycle converts  $^{12}\text{C}$  into  $^{13}\text{C}$ . Since the important factories of  $^{12}\text{C}$  are less massive  $2\text{--}3 M_\odot$  stars, the  $^{13}\text{C}/^{12}\text{C}$  ratio in the ejecta of IMSs is strongly mass-dependent, peaking sharply between 4 to  $5 M_\odot$ . Figure 9 shows the predicted evolution of  $^{13}\text{C}/^{12}\text{C}$  as a function of  $[\text{Fe}/\text{H}]$ . For both the solar and outer radii models, the introduction of an IM-enhanced IMF increases the  $^{13}\text{C}/^{12}\text{C}$  ratio 4–6-fold in the metallicity range corresponding to the greatest enhancement of the heavy Mg isotopes. To estimate the uncertainty in these results due to the stellar yields, we also ran identical models using the LIMS yields from van den Hoek & Groenewegen (1997) and Marigo (2001), depicted with thin dotted and dot-dashed lines, respectively. High values of  $^{13}\text{C}/^{12}\text{C}$  may conflict with the symmetry of C IV line profiles observed in some QSO absorbers and could

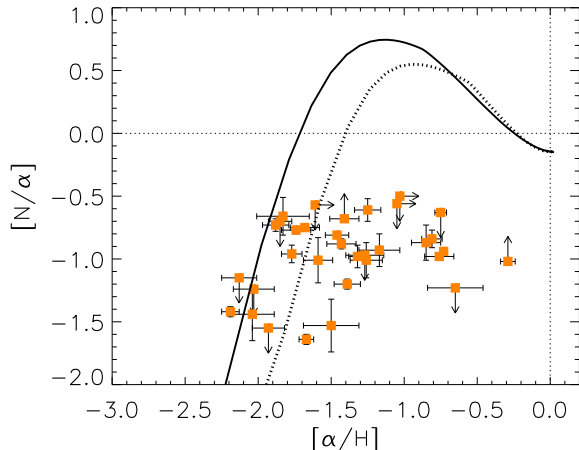


**Figure 7.** Sensitivity of  $[N/\alpha]$  vs  $[\alpha/H]$  to the star formation efficiency. The solid line represents the IM-enhanced solar radius model, as seen in Fig 6. The dotted line shows the effect of increasing star formation (SF) efficiency by a factor of 2.5. Increased SF efficiency improves the agreement with the DLA data (symbols), but still overproduces N at  $[\alpha/H] \sim -1$ .

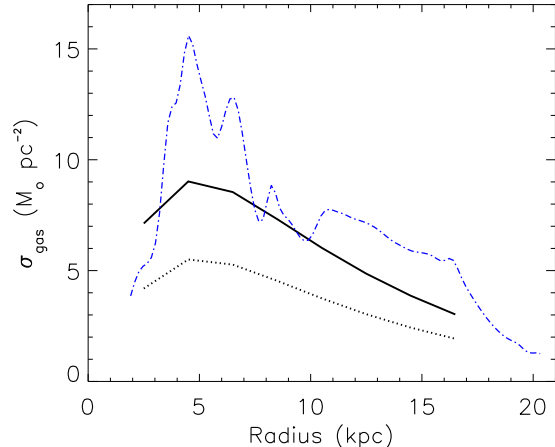


**Figure 8.** Present-day gas surface density profile. The dotted line presents the result for the model with star formation efficiency increased by a factor of 2.5 with respect to the standard model (solid line). The dot-dashed line corresponds to data from Dame (1993) based on observations of atomic and molecular hydrogen. The standard model replicates the observations to within a factor of two, whereas increased star formation efficiency leads to excess depletion of interstellar gas.

impose a further constraint on the shape of the IMF at early times. This will be discussed in more detail in Section 6.

#### 4.5 Silicon, aluminium and phosphorus

Since transitions from Si are important anchor lines in the many-multiplet method, we show the predicted behaviour of  $(^{29}\text{Si}+^{30}\text{Si})/^{28}\text{Si}$  as a function  $[\text{Fe}/\text{H}]$  in Fig. 10. The relative abundance of Si isotopes is not affected by an enhanced early population of AGB stars to the extent of N and the heavy Mg and C isotopes. Indeed,  $(^{29}\text{Si}+^{30}\text{Si})/^{28}\text{Si}$  remains well below the solar value (open square) for both the local and outer disk models (thick lines). Nevertheless, the  $\Delta\alpha/\alpha$  measured in high- $z_{\text{abs}}$  QSO absorption systems

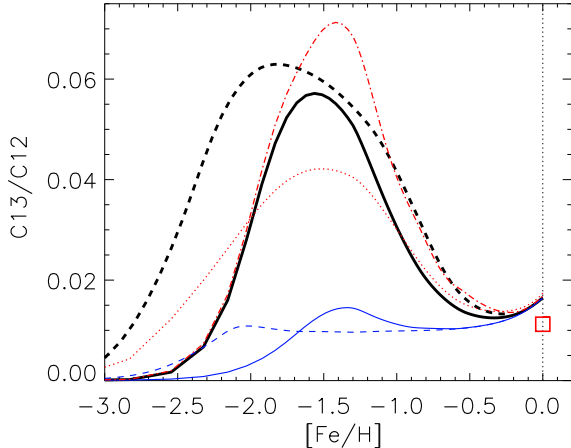


**Figure 9.** Evolution of  $^{13}\text{C}/^{12}\text{C}$  as a function of  $[\text{Fe}/\text{H}]$ . Symbols and lines have the same meaning as in Fig 4. The thin dotted and dot-dashed lines show the IM-enhanced solar radius model in the case of van den Hoek & Groenewegen (1997) and Marigo (2001) IMS yields, respectively.

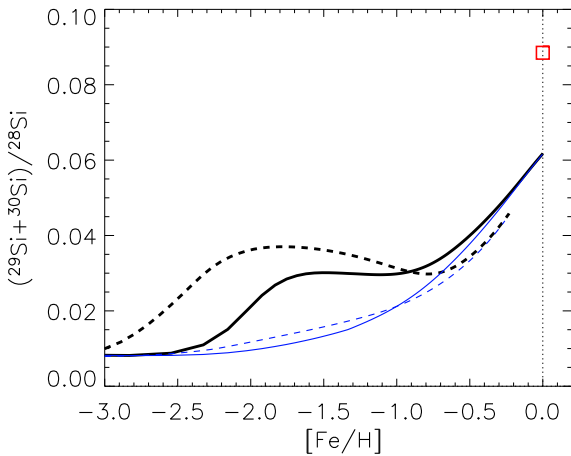


**Figure 10.** Evolution of  $(^{29}\text{Si}+^{30}\text{Si})/^{28}\text{Si}$  as a function of  $[\text{Fe}/\text{H}]$ . Symbols and lines have the same meaning as in Fig 4.

is largely independent of the Si isotopic composition, as highlighted in Section 1.2. Thus, even a dramatic elevation in  $(^{29}\text{Si}+^{30}\text{Si})/^{28}\text{Si}$  due to AGB stars would not account for the high-redshift results from MFW04.

Aluminium is another element whose production by AGB stars is expected to be important (e.g. Karakas & Lattanzio 2003). The synthesis of Al via the Mg-Al chain is particularly efficient in metal-poor  $4-6\text{ M}_\odot$  stars. The evolution of  $[\text{Al}/\text{Fe}]$  with  $[\text{Fe}/\text{H}]$  in the ISM is depicted in Fig. 11. Observations of Al in both DLAs (solid squares) and nearby stars (circles and open squares) covering a wide range of metallicities make this element a potentially useful discriminant of the different IMF models. Unfortunately, most of the DLA measurements are lower limits, owing to line saturation (Prochaska & Wolfe 2002). The normal IMF models (thin lines) pass through the lowermost DLA detections, but only the IM-enhanced IMF models (thick lines) can satisfy the highest DLA upper limits. The power of Al to constrain the shape of the early IMF is diminished by the inability of either solar radius model to match the stellar observations at high and low metallicity. The over-

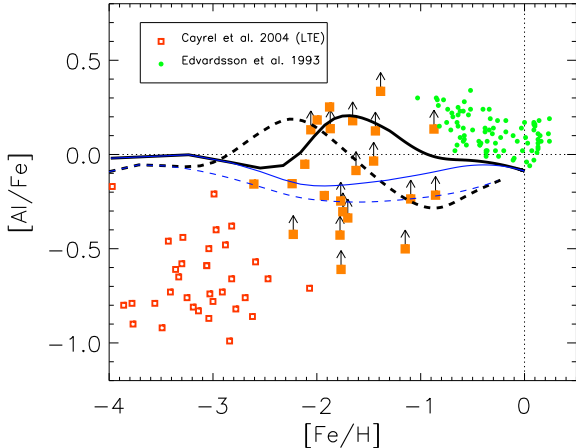


**Figure 11.** Variation of  $[\text{Al}/\text{Fe}]$  as a function of  $[\text{Fe}/\text{H}]$ . Dashed and solid lines have the same meaning as in Fig 4. DLA measurements from Prochaska et al. are plotted with solid square symbols, while circles and open squares show stellar observations from Edvardsson et al. (1993) and Cayrel et al. (2004), respectively.

production of Al with respect to metal-poor halo stars and the underproduction relative to thin-disk stars is a problem of standard Galactic chemical evolution models that has been noted by other authors (e.g. Timmes et al. 1995; Alibés et al. 2001). However, we note that local thermodynamic equilibrium (LTE) calculations underestimate the Al abundance in metal-poor stars. The open squares in Fig. 11 would be about 0.6 dex higher if non-LTE effects were included (e.g. Gehren et al. 2004).

The production of phosphorus from IMSs leads to a  $\sim 0.5$  dex increase in  $[\text{P}/\text{Fe}]$  when the IM-bump is added to the standard IMF, as shown in Fig. 12. Stars in the  $4-6\text{ M}_\odot$  mass range are the chief culprits for the additional  $^{31}\text{P}$ , which is understood to be generated through neutron-capture onto Si followed by  $\beta$ -decay to  $^{31}\text{P}$  (J. Lattanzio, private communication). As is the case for Al, the difference between the two IMF models is significant, but the DLA measurements do not allow the elimination of either scenario. In the case of P, the DLA data is very scant and consists mostly of upper limits since the  $\text{P}\,\text{II}$  line is often blended in the  $\text{Ly}\alpha$  forest (Dessauges-Zavadsky et al. 2004). Nevertheless, we present our predictions for Al and P in the event that the growing collection of DLA measurements may eventually provide a more stringent test of the models presented in this paper.

## 4.6 Uncertainties

### 4.6.1 Magnesium

Denissenkov & Herwig (2003) and Denissenkov & Weiss (2004) showed that the production of  $^{25}\text{Mg}$  and  $^{26}\text{Mg}$  in a typical  $5\text{ M}_\odot$  AGB star is fairly robust to the number of thermal-pulses, the HBB temperature, and the third dredge-up efficiency. The final envelope abundance of  $^{25}\text{Mg}$  and  $^{26}\text{Mg}$  in their series of models agreed within  $\sim 0.1$  dex and  $\sim 0.2$  dex, respectively. Fenner et al. (2004) estimated the sensitivity of the AGB yields of  $^{25}\text{Mg}$  and  $^{26}\text{Mg}$  to the mass-loss prescription, finding them reduced by  $\sim 0.2$  dex when the Vassiliadis & Wood (1993) mass-loss law was replaced with a steadier rate from Reimers (1975) (with  $\eta = 3.5$  on the AGB). The treatment of convection in AGB models has recently been investigated by Ventura (2004), who found that the yields were very

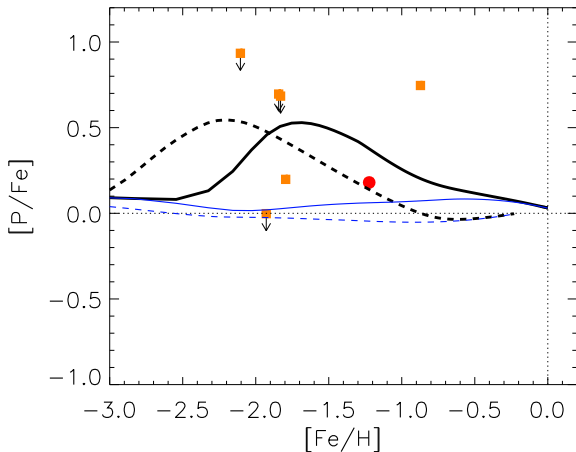


**Figure 12.** Variation of [P/Fe] as a function of [Fe/H]. Dashed and solid lines have the same meaning as in Fig. 4. DLA measurements from Prochaska et al. are plotted with square symbols, while the circle is from Outram, Chaffee, & Carswell (1999).

sensitive to the adoption of standard mixing length theory (MLT) versus the full spectrum of turbulence (FST) model. The latter case results in greater mass-loss rates, shorter AGB lifetimes, less third dredge-up, and reduced yields of heavy elements including CNO and the Mg isotopes. The FST model faces serious hurdles of its own, since it predicts a deficit of Na in AGB ejecta and a *positive* O-Na correlation: at odds with observations of globular cluster stars believed to be polluted by AGBs (Ventura, D'Antona, & Mazzitelli 2004).

A further uncertainty relates to the presence of a  $^{13}\text{C}$  pocket, which is neglected in the AGB models implemented in this study. One might expect that the inclusion of this additional source of neutrons would increase the production of  $^{25}\text{Mg}$  and  $^{26}\text{Mg}$ . However the impact of a  $^{13}\text{C}$  pocket on nucleosynthesis in metal-poor IMS should be marginal in comparison to the effects of HBB (M. Lugaro, *private communication*). Despite these unknowns, the ability of our standard Galactic chemical evolution model to reproduce the Mg isotopic ratios in metal-poor stars by adding in the Karakas & Lattanzio (2003) yields, suggests that their Mg predictions are reasonably accurate.

The total production of  $^{25,26}\text{Mg}$  with respect to  $^{24}\text{Mg}$  from Type II SNe is uncertain to a similar degree due to internal uncertainties in the stellar models as well as sensitivity to the shape and upper mass limit of the IMF. Fenner et al. (2003) found that a Salpeter (1955) IMF leads to 50 per cent higher present-day  $^{26}\text{Mg}/^{24}\text{Mg}$  ratio than in the case of a Kroupa et al. (1993) function, because the Salpeter law gives rise to a greater fraction of massive stars (see their figs. 5 and 6). The shaded region in Fig. 5 indicates the  $\pm 0.2$  dex uncertainty in the results due to errors in both the AGB and SN II contribution.

#### 4.6.2 Nitrogen and $^{13}\text{C}/^{12}\text{C}$

To estimate the uncertainty in the predicted evolution of N and the  $^{13}\text{C}/^{12}\text{C}$  ratio, we ran identical models using two alternative sets of IMS yields: those of van den Hoek & Groenewegen (1997) and Marigo (2001). The Marigo yields for N were in close agreement with those of Karakas & Lattanzio (2003) while the implementation of the van den Hoek & Groenewegen (1997) yields produced

even more N. The dotted line in Fig. 6 displays the results from an IM-enhanced solar radius model using the van den Hoek & Groenewegen (1997) yields in place of Karakas et al. (i.e. compare dotted with thick solid curve). It is clear that the problem of excess nitrogen is further exacerbated in this case.

The dotted and dot-dashed lines in Fig. 9 show the behaviour of  $^{13}\text{C}/^{12}\text{C}$  assuming van den Hoek & Groenewegen (1997) and Marigo (2001) IMS yields, respectively. The Marigo yields generate the highest  $^{13}\text{C}/^{12}\text{C}$  peak [with  $(^{13}\text{C}/^{12}\text{C})_{\text{max}} = 0.073$ ] and those of van den Hoek & Groenewegen (1997) the lowest [with  $(^{13}\text{C}/^{12}\text{C})_{\text{max}} = 0.042$ ]. The region encompassed by these two extreme models is indicative of the level of uncertainty afflicting the models.

## 5 DISCUSSION

### 5.1 Summary of Results

Murphy et al. (2001b) pointed out that  $\Delta\alpha/\alpha$  measurements are sensitive to the isotopic composition of Mg in the gas-phase of the low- $z$  absorbers used in varying- $\alpha$  studies. Standard models of chemical evolution predict that the abundance of the neutron-rich isotopes of Mg relative to  $^{24}\text{Mg}$  decreases with lookback time, making the MFW04  $\Delta\alpha/\alpha$  result even more significant. However, AMO04 demonstrated that a sufficiently enhanced early population of intermediate-mass stars can raise  $(^{25}\text{Mg}+^{26}\text{Mg})/^{24}\text{Mg}$  to the supersolar levels needed to render the MFW04  $\Delta\alpha/\alpha$  result null.

A major problem with this scenario is the almost inevitable overproduction of N when compared against the DLA data (Fig. 6). This is because the AGB stars responsible for significant  $^{25,26}\text{Mg}$  production are also important sources of N. There are various ways to reconcile an IM-enhanced IMF with the low N abundances in DLAs, but none are entirely satisfactory. For instance, since nucleosynthesis within very metal-poor IMSs is not well understood, the theoretical N yields may be overestimated. However, in this case, it would be difficult to explain the high N abundance found in some of the most iron-depleted stars in our galaxy (e.g. Norris, Beers & Ryan 2000; Christlieb et al. 2004). Another way to mitigate the problem of excess  $[\text{N}/\alpha]$  is through increased star formation efficiency, however this leads to severe gas depletion that may be inconsistent with the gas-rich nature of DLAs (Fig. 8). Finally, the history of many DLAs may be marked by periods of supernova-driven outflows, but it is not clear how such galactic winds could preferentially remove N but not the heavy Mg isotopes. Thus, the observed N abundance in QSO absorbers still stands as a robust test of a putative IM-enhanced early IMF.

The enhanced  $^{13}\text{C}/^{12}\text{C}$  ratio predicted by these types of chemical evolution models (Fig. 9) holds promise as a future probe of the AGB contribution to QSO absorption line abundances. Carlsson et al. (1995) has calculated the isotopic shifts in the ubiquitous C IV  $\lambda 1548/1550$  alkali doublet, finding the  $^{14}\text{C}$  line to lie  $\Delta v = 10.3 \text{ km s}^{-1}$  to the blue of the  $^{12}\text{C}$  line. Recent calculations by Berengut et al. (in preparation) confirm these large shifts to within 1 per cent precision and show the  $^{13}\text{C}-^{12}\text{C}$  separation to be  $\Delta v = 5.5 \text{ km s}^{-1}$ . Enhancements as large as  $^{13}\text{C}/^{12}\text{C} \approx 0.1$  may already be ruled out by the symmetric C IV line profiles observed in  $R \gtrsim 45\,000$  ( $\text{FWHM} \lesssim 6.7 \text{ km s}^{-1}$ ) spectra of highly ionized QSO absorbers with simple velocity structure (e.g. Petitjean & Aracil 2004). However, placing limits at lower  $^{13}\text{C}$  abundances may be unconvincing unless the laboratory wavelengths of the C IV doublet transitions can be measured with better precision than  $0.4 \text{ km s}^{-1}$

(Griesmann & Kling 2000). If the calculated isotopic separations for transitions of other C species (e.g. C I and C II) prove to be as large as those for C IV, they may provide a more reliable probe of the  $^{13}\text{C}/^{12}\text{C}$  ratio in gas more closely related to DLAs and, therefore, the chemical evolution models presented here.

Given that many QSO absorbers are thought to probe slowly evolving systems such as dwarf galaxies and the outer regions of galactic disks, we simulated chemical evolution at large galactocentric radii, where metal-enrichment is more gradual. We found that the chemical signature from an enhanced IMS population at low metallicities was more pronounced in the outer disk, with respect to the solar neighbourhood. This follows directly from the assumed metallicity-dependence of the IMS enhancement. Thus, our IM-enhanced models predict that systems with the slowest build-up of metals will bear the strongest signature of AGB-pollution.

The chemical abundance constraints imposed by QSO absorption systems do not support excess numbers of AGB stars being formed in the types of systems from which MFW04 derived a varying  $\alpha$ . Moreover, a significantly enhanced AGB population in the local Galaxy is ruled out by the sub-solar ratios of the neutron-rich Mg isotopes to  $^{24}\text{Mg}$  in nearby metal-poor stars. We now summarise other arguments for and against the IMF having a non-standard shape in the early universe.

## 5.2 Other arguments for and against an early, IM-enhanced IMF

### 5.2.1 Observations of deuterium, carbon and nitrogen

Motivated by the large observed scatter and possible trends with metallicity of local and high- $z_{\text{abs}}$  D abundance determinations, Fields et al. (2001) and Prantzos & Ishimaru (2001) speculated that D could be destroyed within stars without an accompanying increase in metals, provided that: (i) the earliest populations of stars were strongly enhanced in IMSs, and (ii) zero-metallicity IMSs do not release their synthesized C and N. Prantzos & Ishimaru (2001) emphasize that if the second provision is not met, C and N abundances should be highly enhanced in high- $z_{\text{abs}}$  systems if their D has been depleted through astration alone. They note that this is inconsistent with the DLA data. Indeed, based on the  $\text{N}/\alpha$  trend in DLAs, Prochaska et al. (2002) presented a case for a top-heavy IMF, with the birth of IMSs actually *suppressed* in many QSO absorption systems.

The abundance of C and N in Galactic stars and DLAs provides one of the strongest constraints on any enhancement in the population of LIMS in the early Galaxy (Gibson & Mould 1997; Fields, Freese, & Graff 2000). However, this is contingent upon how much C and N is released by extremely metal-poor IMSs. Fujimoto et al. (2000) provide evidence favouring the suppression of C and N yields from zero-metallicity IMSs, whereas Chieffi et al. (2001) reach the opposite conclusion. Abia et al. (2001) propose that an early IMF peaked between  $3-8 M_{\odot}$  helps explain the presence of metal-poor Galactic stars with enhanced C and N abundances, presuming that LIMS release C and N in large quantities. Thus, the stellar models do not offer a cohesive picture of the level of C and N enrichment from metal-poor LIMS, nor do observations of DLAs and metal-poor stars clarify the situation. However, if AGBs are responsible for  $^{25,26}\text{Mg}$  enhancements large enough to mimic a varying  $\alpha$  in the redshift range  $0.5 \lesssim z_{\text{abs}} \lesssim 1.8$ , they will tend to have had a much higher initial metallicity than primordial. Thus, their yields are not subject to the very large uncertainties afflicting zero-metallicity models.

### 5.2.2 White dwarfs

Evidence from microlensing surveys initially led to speculation that white dwarf remnants contribute up to half of the mass of the Milky Way halo (e.g. Bennett et al. 1996; Alcock et al. 1995). Populating the halo with such a large fraction of white dwarfs requires the early IMF to be heavily biased toward stars with initial mass in the range  $1-8 M_{\odot}$ . Adams & Laughlin (1996) constructed IMFs capable of producing a white-dwarf dominated halo, and AMO04 adopted IMF parameters that were consistent with their deduced constraints. However, the white dwarf contribution to the dynamical mass of the Galactic halo has since been drastically revised downwards to less than a few percent (Gibson & Mould 1997; Flynn, Holopainen & Holmberg 2003; Garcia-Berro et al. 2004; Lee et al. 2004), obviating the need to invoke non-standard IMFs.

### 5.2.3 Theoretical star formation

Theoretical models of star formation suggest that the IMF of primordial gas would be biased toward higher mass stars (e.g. Abel, Bryan & Norman 2000; Kroupa 2001; Hernandez & Ferrara 2001; Mackey, Bromm & Hernquist 2003; Clarke & Bromm 2003). This is due to diminished cooling efficiency in metal-poor gas. However, recent hydrodynamical simulations of the collapse and fragmentation of primordial gas have predicted bimodal primordial IMFs with peaks at about  $100$  and  $1 M_{\odot}$  (Nakamura & Umemura 2001) and  $30$  and  $0.3 M_{\odot}$  (Omukai & Yoshii 2003).

### 5.2.4 Extragalactic observations

Empirical support exists for an early IMF skewed toward high stellar masses in extragalactic environments. For instance, to explain the high metal content of the intra-cluster medium various top-heavy IMFs have been proposed (e.g. Gibson & Matteucci 1997; Elbaz, Arnaud & Vangioni-Flam 1995). The photometric properties of ellipticals have also been well-explained assuming a top-heavy IMF (Arimoto & Yoshii 1987). AMO04 note that their model is not inconsistent with the notion of a very early population of very massive stars that enrich the ISM to  $Z \sim 10^{-3}$ .

In light of the uncertainties besetting theoretical simulations of star formation and the interpretation of extragalactic photometric data, careful analysis of the nucleosynthetic enrichment patterns of QSO absorption systems may be a vital step in deciphering the shape of the IMF in different astrophysical environments.

## 6 CONCLUSIONS

An early IMF heavily biased towards intermediate-mass stars is a potential explanation of the  $\alpha$ -variation apparent in Keck/HIRES QSO spectra. During their AGB phase these stars produce large quantities of  $^{25,26}\text{Mg}$  which later pollute QSO absorption systems at  $z_{\text{abs}} \lesssim 1.8$ , causing an apparent shift in the Mg absorption lines and a spurious  $\Delta\alpha/\alpha < 0$ . However, such a strong contribution from AGBs should be evident in the detailed abundance patterns obtained in a growing number of DLAs. Using chemical evolution models of a Milky Way-like spiral galaxy at different radii, we have tested the idea that AGB stars were more prevalent in the metal-poor Universe. The predicted chemical ramifications of an enhanced AGB population are not supported by the available data, with the strongest argument against severe AGB pollution coming from the low  $[\text{N}/\alpha]$  values observed in DLAs. Contrary to the

conclusions of AM004, we do not find consistent model parameters which simultaneously explain the Keck/HIRES varying- $\alpha$  and abundance data. We also contend that a variety of other arguments for invoking an IM-enhanced IMF are, at best, unclear. Future measurements of (or limits on) the  $^{13}\text{C}/^{12}\text{C}$  ratio from line-profile asymmetries and further DLA observations of other elements synthesised by AGB stars, such as Al and P, may provide additional constraints on the IMF's shape at early epochs.

The sensitivity of low- $z$  Mg/Fe  $\Delta\alpha/\alpha$  measurements to isotopic abundance variations in Mg (Fig. 1) and the clear link to the nucleosynthetic history of QSO absorbers demonstrates the importance of careful  $\Delta\alpha/\alpha$  measurements, even in the absence of real variations in  $\alpha$ . If  $\Delta\alpha/\alpha$  is measured to be zero in  $z_{\text{abs}} \lesssim 1.8$  absorbers via independent means (e.g. by combining H $\alpha$  21-cm and molecular absorption lines; Darling 2003) then future samples of Mg/Fe absorbers might reveal Mg isotopic abundance variations in two ways: (i) through the bulk relative line shifts between Mg and Fe transitions studied previously and, (ii) if we assume that AGB pollution of the absorbers is not uniform, through an increased scatter in the line shifts. Note that no increased scatter is observed in the current HIRES or UVES samples (MFW04; Chand et al. 2004a).

## ACKNOWLEDGEMENTS

The authors are extremely grateful to Maria Lugaro and Amanda Karakas for many valuable discussions. We thank the anonymous referee for comments that helped improve this paper. Financial support from the Australian Research Council (ARC) is gratefully acknowledged. We also acknowledge the Monash Cluster Computing Laboratory, the Victorian Partnership for Advanced Computing and the Australian Partnership for Advanced Computing for use of supercomputing facilities. MTM thanks PPARC for support at the IoA under the observational rolling grant. YF thanks the AFUW-SA for their support through the Daphne Elliot Bursary.

## REFERENCES

Abel, T., Bryan, G. L., & Norman, M. L. 2000, *ApJ*, 540, 39  
 Abia, C., Domínguez, I., Straniero, O., Limongi, M., Chieffi, A., & Isern, J. 2001, *ApJ*, 557, 126  
 Adams, F. C. & Laughlin, G. 1996, *ApJ*, 468, 586  
 Alcock, C., et al. 1995, *Phys. Rev. Lett.*, 74, 2867  
 Alibés, A., Labay, J., & Canal, R. 2001, *A&A*, 370, 1103  
 Arimoto, N. & Yoshii, Y. 1987, *A&A*, 173, 23  
 Ashenfelter T. P., Mathews G. J., Olive K. A., 2004a, *Phys. Rev. Lett.*, 92, 041102  
 Ashenfelter T. P., Mathews G. J., Olive K. A., 2004b, *ApJ*, 615, 82  
 Bethe H. A., Salpeter E. E., 1977, *Quantum mechanics of one- and two-electron atoms*. Plenum, New York, NY, USA  
 Bennett, D. P., et al. 1996, *ASP Conf. Ser.* 88: Clusters, Lensing, and the Future of the Universe, 95  
 Berengut J. C., Dzuba V. A., Flambaum V. V., 2003, *Phys. Rev. A*, 68, 022502  
 Carlsson J., Jonsson P., Godefroid M. R., Fischer C. F., 1995, *J. Phys. B*, 28, 3729  
 Cayrel, R., et al. 2004, *A&A*, 416, 1117  
 Centurión, M., Molaro, P., Vladilo, G., Péroux, C., Levshakov, S. A., & D'Odorico, V. 2003, *A&A*, 403, 55  
 Chand H., Petitjean P., Srianand R., Aracil B., 2004b, *A&A*, 430, 47  
 Chand H., Srianand R., Petitjean P., Aracil B., 2004a, *A&A*, 417, 853  
 Chiappini, C., Matteucci, F., & Gratton, R. 1997, *ApJ*, 477, 765  
 Chieffi, A., Domínguez, I., Limongi, M., & Straniero, O. 2001, *ApJ*, 554, 1159  
 Christlieb, N., Gustafsson, B., Korn, A. J., Barklem, P. S., Beers, T. C., Bessell, M. S., Karlsson, T., & Mizuno-Wiedner, M. 2004, *ApJ*, 603, 708  
 Clarke, C. J. & Bromm, V. 2003, *MNRAS*, 343, 1224  
 Cowie L. L., Songaila A., 1995, *ApJ*, 453, 596  
 Dame, T. M. 1993, *AIP Conf. Proc.* 278: Back to the Galaxy, 278, 267  
 Darling J., 2003, *Phys. Rev. Lett.*, 91, 011301  
 Denissenkov, P. A. & Herwig, F. 2003, *ApJL*, 590, L99  
 Denissenkov, P. A. & Weiss, A. 2004, *ApJ*, 603, 119  
 Dessauges-Zavadsky, M., Calura, F., Prochaska, J. X., D'Odorico, S., & Matteucci, F. 2004, *A&A*, 416, 79  
 Dirac P. A. M., 1937, *Nat*, 139, 323  
 Drullinger R. E., Wineland D. J., Bergquist J. C., 1980, *Appl. Phys.*, 22, 365  
 Dzuba V. A., Flambaum V. V., Webb J. K., 1999a, *Phys. Rev. A*, 59, 230  
 Dzuba V. A., Flambaum V. V., Webb J. K., 1999b, *Phys. Rev. Lett.*, 82, 888  
 Edvardsson, B., Andersen, J., Gustafsson, B., Lambert, D. L., Nissen, P. E., & Tomkin, J. 1993, *A&A*, 275, 101  
 Elbaz, D., Arnaud, M., & Vangioni-Flam, E. 1995, *A&A*, 303, 345  
 Fenner, Y. & Gibson, B. K. 2003, *Publ. Astron. Soc. Aust.*, 20, 189  
 Fenner, Y., Gibson, B. K., Lee, H.-c., Karakas, A. I., Lattanzio, J. C., Chieffi, A., Limongi, M., & Yong, D. 2003, *Publ. Astron. Soc. Aust.*, 20, 340  
 Fenner, Y., Prochaska, J. X., & Gibson, B. K. 2004, *ApJ*, 606, 116  
 Fenner, Y., Campbell, S., Karakas, A. I., Lattanzio, J. C., & Gibson, B. K. 2004, *MNRAS*, 280  
 Fields, B. D., Freese, K., & Graff, D. S. 2000, *ApJ*, 534, 265  
 Fields, B. D., Mathews, G. J., & Schramm, D. N. 1997, *ApJ*, 483, 625  
 Fields, B. D., Olive, K. A., Silk, J., Cassé, M., & Vangioni-Flam, E. 2001, *ApJ*, 563, 653  
 Flynn, C., Holopainen, J., & Holmberg, J. 2003, *MNRAS*, 339, 817  
 Fujimoto, M. Y., Ikeda, Y., & Iben, I. J. 2000, *ApJL*, 529, L25  
 García-Berro, E., Torres, S., Isern, J., & Burkert, A. 2004, *A&A*, 418, 53  
 Gay P. L., Lambert D. L., 2000, *ApJ*, 533, 260  
 Gehren, T., Liang, Y. C., Shi, J. R., Zhang, H. W., & Zhao, G. 2004, *A&A*, 413, 1045  
 Gibson, B. K., Giroux, M. L., Penton, S. V., Stocke, J. T., Shull, J. M., & Tumlinson, J. 2001, *AJ*, 547, 3280  
 Gibson, B. K. & Matteucci, F. 1997, *MNRAS*, 291, L8  
 Gibson, B. K. & Mould, J. R. 1997, *ApJ*, 482, 98  
 Goswami, A. & Prantzos, N., 2000, *A&A*, 359, 191  
 Gratton, R. G., Carretta, E., Claudi, R., Lucatello, S., & Barbieri, M., 2003, *A&A*, 404, 187  
 Gregg, L. & Renzini, A. 1983, *A&A*, 118, 217  
 Griesmann U., Kling R., 2000, *ApJ*, 536, L113  
 Hallstadius L., 1979, *Z. Phys. A*, 291, 203  
 Hernandez, X. & Ferrara, A. 2001, *MNRAS*, 324, 484  
 Iwamoto, K., Brachwitz, F., Nomoto, K., Kishimoto, N., Umeda, H., Hix, W. R., & Thielemann, F. 1999, *ApJS*, 125, 439  
 Karakas, A. I. & Lattanzio, J. C. 2003, *Publ. Astron. Soc. Aust.*, 20, 279  
 Kobayashi, C., Tsujimoto, T., & Nomoto, K. 2000, *ApJ*, 539, 26  
 Kozlov M. G., Korol V. A., Berengut J. C., Dzuba V. A., Flambaum V. V., 2004, *Phys. Rev. A*, 70, 062108  
 Kroupa, P., Tout, C. A., & Gilmore, G. 1993, *MNRAS*, 262, 545  
 Kroupa, P., 2001, *MNRAS*, 322, 231  
 Lee, H., Gibson, B. K., Fenner, Y., Brook, C. B., Kawata, D., Renda, A., Holopainen, J., & Flynn, C. 2004, *Publ. Astron. Soc. Aust.*, 21, 153  
 Levshakov S. A., Centurion M., Molaro P., D'Odorico S., 2004, *A&A*, submitted, preprint (astro-ph/0408188)  
 Mackey, J., Bromm, V., & Hernquist, L. 2003, *ApJ*, 586, 1  
 Marigo, P. 2001, *A&A*, 370, 194  
 Matteucci, F. & Gregg, L. 1986, *A&A*, 154, 279  
 Milne E. A., 1935, *Relativity, Gravitation and World Structure*. Clarendon Press, Oxford, UK  
 Milne E. A., 1937, *Proc. R. Soc. A*, 158, 324  
 Murphy M. T., Flambaum V. V., Webb J. K., Dzuba V. V., Prochaska J. X., Wolfe A. M., 2004, *Lecture Notes Phys.*, 648, 131  
 Murphy M. T., Webb J. K., Flambaum V. V., 2003, *MNRAS*, 345, 609

Murphy M. T., Webb J. K., Flambaum V. V., Churchill C. W., Prochaska J. X., 2001b, MNRAS, 327, 1223

Murphy M. T., Webb J. K., Flambaum V. V., Dzuba V. A., Churchill C. W., Prochaska J. X., Barrow J. D., Wolfe A. M., 2001a, MNRAS, 327, 1208

Murphy M. T., Webb J. K., Flambaum V. V., Prochaska J. X., Wolfe A. M., 2001c, MNRAS, 327, 1237

Nakamura, F. & Umemura, M. 2001, ApJ, 548, 19

Norris, J. E., Beers, T. C., & Ryan, S. G. 2000, ApJ, 540, 456

Omukai, K. & Yoshii, Y. 2003, ApJ, 599, 746

Outram, P. J., Chaffee, F. H., & Carswell, R. F. 1999, MNRAS, 310, 289

Pagel, B. E. J. 2001, PASP, 113, 137

Petitjean P., Aracil B., 2004b, A&A, 422, 523

Pettini, M., Ellison, S. L., Steidel, C. C., & Bowen, D. V. 1999, ApJ, 510, 576

Pickering J. C., Thorne A. P., Webb J. K., 1998, MNRAS, 300, 131

Prantzos, N. & Ishimaru, Y. 2001, A&A, 376, 751

Prochaska, J. X. & Wolfe, A. M. 2002, ApJ, 566, 68

Prochaska, J. X., Henry, R. B. C., O'Meara, J. M., Tytler, D., Wolfe, A. M., Kirkman, D., Lubin, D., & Suzuki, N. 2002, PASP, 114, 933

Quast R., Reimers D., Levshakov S. A., 2004b, A&A, 415, L7

Reimers, D. 1975, Memoires of the Societe Royale des Sciences de Liege, 8, 369

Renzini, A. & Voli, M. 1981, A&A, 94, 175

Romano, D., Matteucci, F., Salucci, P. & Chiappini, C. 2000, ApJ, 539, 235

Rosman K. J. R., Taylor P. D. P., 1998, J. Phys. Chem. Ref. Data, 27, 1275

Salpeter, E. E. 1955, ApJ, 121, 161

Schaller, G., Schaerer, D., Meynet, G., & Maeder, A. 1992, A&AS, 96, 269

Schmidt, M. 1959, ApJ, 129, 243

Sembach, K.R., Gibson, B.K., Fenner, Y. & Putman, M.E. 2002, ApJ, 572, 178

Shetrone, M. D., Côté, P., & Sargent, W. L. W. 2001, ApJ, 548, 592

Srianand R., Chand H., Petitjean P., Aracil B., 2004, Phys. Rev. Lett., 92, 121302

Thielemann, F.-K., Nomoto, K., & Yokoi, K. 1986, A&A, 158, 17

Timmes F. X., Woosley S. E., Weaver T. A., 1995, ApJS, 98, 617

Tinsley, B.M. 1980, Fund. Cosm. Phys., 5, 287

Uzan J., 2003, Rev. Mod. Phys., 75, 403

van den Hoek, L. B. & Groenewegen, M. A. T. 1997, A&AS, 123, 305

Varshalovich D. A., Panchuk V. E., Ivanchik A. V., 1996, Astron. Lett., 22, 6

Varshalovich D. A., Potekhin A. Y., 1994, Astron. Lett., 20, 771

Varshalovich D. A., Potekhin A. Y., Ivanchik A. V., 2000, in Dunford R. W., Gemmel D. S., Kanter E. P., Kraessig B., Southworth S. H., Young L., eds, AIP Conf. Proc. Vol. 506, X-Ray and Inner-Shell Processes. Argonne National Laboratory, Argonne, IL, USA, p. 503

Vassiliadis, E. & Wood, P. R. 1993, ApJ, 413, 641

Ventura, P. 2004, Memorie della Societa Astronomica Italiana, 75, 654

Ventura, P., D'Antona, F., & Mazzitelli, I. 2004, Memorie della Societa Astronomica Italiana, 75, 335

Wakker B.P. et al., 1999, Nat, 402, 388

Webb J. K., Flambaum V. V., Churchill C. W., Drinkwater M. J., Barrow J. D., 1999, Phys. Rev. Lett., 82, 884

Webb J. K., Murphy M. T., Flambaum V. V., Dzuba V. A., Barrow J. D., Churchill C. W., Prochaska J. X., Wolfe A. M., 2001, Phys. Rev. Lett., 87, 091301

Woosley, S. E. & Weaver, T. A. 1995, ApJS, 101, 181

Yong D., Grundahl F., Lambert D. L., Nissen P. E., Shetrone M. D., 2003a, A&A, 402, 985

Yong D., Lambert D. L., Ivans I. I., 2003b, ApJ, 599, 1357